

Specific-heat measurements in superconducting indium-thallium alloys and the pseudopotential form factor*

Lakshmi V. Munukutla[†] and R. L. Cappelletti

Department of Physics, Ohio University, Athens, Ohio 45701

(Received 31 October 1979)

Normal-state specific heats between 1 and 4.4 K and superconducting transition temperatures of pure indium and In-Tl alloys have been measured. Excellent agreement with previous results was found. $N_{BS}(0)$ was extracted using our γ values and Dynes's λ values and shows a large variation. The measured variation of $\lambda(\omega^2)$ was also obtained from Dynes's results and found to be nearly linear in spite of the large variation of $N_{BS}(0)$. This is shown to be a consequence of the fact that the ratio of the calculated average screened pseudopotential form factor to electron density of states, $\langle v_s^2 \rangle / N_{BS}(0)$, is nearly constant across the alloy series for each element. No anomaly was found in the specific heat of $In_{0.69}Tl_{0.31}$ at the expected martensitic transition temperature.

I. INTRODUCTION

The indium-thallium alloy system is particularly attractive to investigate because of several interesting features. The phase diagram¹ of the alloy indicates solid solutions at all concentrations of many of the basic metallic crystallographic phases: fct, fcc, bcc, and hcp in that order from In to Tl. Tl appears below In in the III A column of the Periodic Table and several properties of the elements and alloys have been well studied.^{2,3} In particular the superconducting transition temperatures, T_c , of bulk alloy samples were magnetically measured by Merriam *et al.*² who also gave some evidence for an interesting martensitic distortion of the fcc to fct phase occurring at around 3 K. Dynes³ has made very detailed tunneling measurements on thin-film superconducting samples in each crystal modification and extracted most of the important information for studying the parameters determining T_c . His calculation of T_c using these parameters and McMillan's⁴ equation show good agreement with experiment.

Both In and Tl are nearly free-electron p -band metals for which a pseudopotential formulation has been found useful in describing several properties.⁵ The electron-phonon interaction has also been so formulated and this alloy system provides a suitable field for observing its variation. To do so requires knowledge of the electron density of states at the Fermi energy, $N(0)$, in addition to the parameters obtained by Dynes. Surprisingly, there were no published reports of measurements from which $N(0)$ could be extracted. In this work we measure T_c and specific heats at low temperatures in bulk In-Tl alloys spanning all the crystal phases. We obtain the electronic specific-heat coefficient γ and Debye temperature Θ_D . Using Dynes's measured values of the electron-phonon parameter λ , we obtain the band-

structure density of states $N_{BS}(0)$. Further, we obtain information on the behavior of an average of the screened pseudopotential form factor $\langle v_s^2 \rangle$ which is compared to calculations of the same. Finally we remark upon our attempts to observe the martensitic distortion in the specific heat of one of the alloys.

II. EXPERIMENT

$In_{1-x}Tl_x$ samples of compositions given in Table I were prepared from MARZ-grade material obtained from Materials Research Corporation (indium) and 99.999% material from Cominco American Incorporated (thallium). The starting materials were first chemically cleaned using hot $HCl:HNO_3 = 3:1$ by volume for indium and dilute nitric acid for thallium. The required amount of each component of the alloy was placed into a well-cleaned Pyrex tube. The alloy components were melted under vacuum of $\leq 10^{-6}$ Torr and agitated well in the molten state to avoid gas pockets and to get better homogeneity. The Pyrex tube with the alloy was sealed under vacuum and the sample allowed to solidify into a cylinder 2 in. long by 0.5 in. diam. The end portions of the cast metal were cut off, so that the sample would fit into the sample holder. The samples were annealed at temperatures very close to their respective melting points under a vacuum of $\leq 10^{-6}$ Torr. Two samples, $In_{0.30}Tl_{0.70}$ and $In_{0.10}Tl_{0.90}$, were quenched and stored in liquid nitrogen immediately following annealing in order to preserve the crystallographic phase characteristic of the annealing temperature.

T_c 's of the annealed samples were measured using an ac susceptibility method. The real part of the ac permeability μ' was measured as a function of temperature in a weak alternating magnetic field of about 1 mOe near the superconducting transition. The

TABLE I. Experimental results. The parameters are discussed in the text.

Thallium conc.	Crystal phase	T_c (K)	γ (mJ/mole K ²)	Θ_D (K)	α (mJ/mole K ⁶)	$\frac{\Delta c}{\gamma T_c} \Big _{T_c}$
0	fcc	3.405 ± 0.003 3.41 ± 0.03 ^a	1.586 ± 0.18	108 ± 0.5	0.0051	1.89 ± 0.12
0.10	fcc	3.276 ± 0.002 3.25 ± 0.03 ^a	1.619 ± 0.21	101 ± 1	0.0059	1.54 ± 0.14
0.31	fcc	3.286 ± 0.03 ^a	5.169 ± 0.3	86 ± 0.3	...	0.77 ± 0.14
0.35	fcc	3.129 ± 0.002	3.738 ± 0.77	92 ± 2	0.00097	
0.70	bcc	3.774 ± 0.002	6.02 ± 2.1	75 ± 1	...	
0.90	hcp	2.945 ± 0.01 (hcp 96%) 3.118 ± 0.015 (bcc 4%)	2.669 ± 0.15	86 ± 0.6	0.005	
1.00 ^b	hcp	2.38	1.47 ± 0.02	78.5 ± 0.2		1.50

^a T_c from specific heat.^bReference 8.

temperature corresponding to the midpoint of the transition was taken as T_c and the temperature difference corresponding to $\frac{1}{4}$ and $\frac{3}{4}$ of the full transition was taken as the width of the transition. A doped germanium resistor was used as the thermometer. This thermometer was calibrated against one supplied by Cryocal Inc., and also by using ⁴He vapor pressure thermometry between 2 and 4 K. Both the apparatus and the calibration of the thermometer were checked by measuring the transition temperature of the pure indium sample, which was found to have $T_c = 3.405 \pm 0.002$ K, in good agreement with $T_c = 3.404 \rightarrow 3.405$ K of Merriam *et al.*² and $T_c = 3.407 \pm 0.001$ K of Finnemore and Mapother.⁶

Heat-capacity measurements were made using the standard heat pulse technique. A schematic drawing of the apparatus is shown in Fig. 1. Heat capacities at constant pressure were measured for all the samples in the normal state and for some samples in the superconducting state also. Heat-capacity measurements in the normal state of the samples were made in a magnetic field of about 408 Oe which was obtained from a nitrogen-cooled 6th-order Garret solenoid. The apparatus and the thermometer were checked by measuring the heat capacity of the pure indium sample and the data obtained in the normal state were in excellent agreement with that of Bryant and Keesom⁷ (shown in Fig. 3).

The primary thermometer used during the heat-capacity measurements was a doped germanium resistor obtained from Cryocal Inc. Two carbon composition resistors were used as secondary thermometers during the measurements. A $\frac{1}{8}$ -W Allen Bradley resistor of nominal value 47 Ω was used for the temperature range of 4.5–2 K and a $\frac{1}{2}$ -W Speer resistor

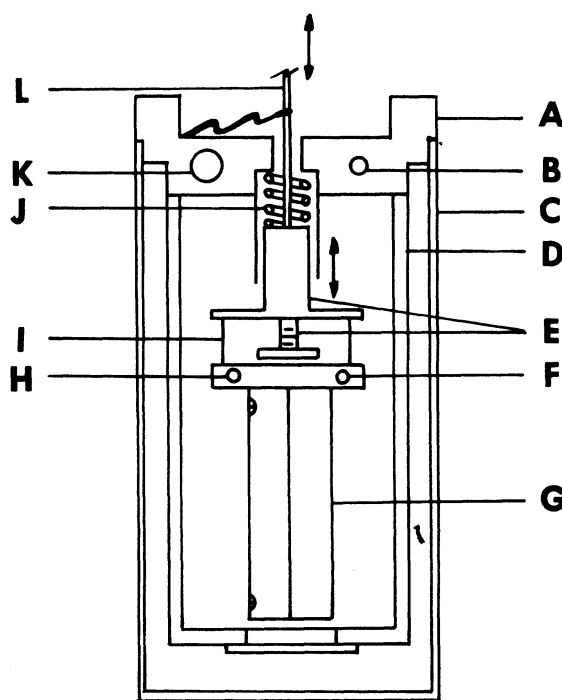


FIG. 1. Specific-heat cryostat (schematic). The part shown is surrounded by a vacuum jacket immersed in 4.2 K He. (A) Copper block which attaches to ⁴He pot; (B) Ge thermometer; (C) radiation shield; (D) copper frame; (E) heat switch plunger; (F) carbon thermometer; (G) copper sample holder; (H) manganin heater; (I) cotton support threads; (J) Be-Cu spring; (K) vapor pressure bulb; (L) thermally anchored heat switch activator running to outside.

of nominal value 470 Ω was used below 2 K. Both the thermometers were calibrated against the primary thermometer in the presence of magnetic field of about 408 Oe during each run. The primary thermometer calibration was checked using ^4He vapor pressure thermometry in the temperature range 4–2 K with T_{58} temperature scale.

III. RESULTS

The superconducting transition of $\text{In}_{0.3}\text{Tl}_{0.7}$ ($x=0.7$) is shown in Fig. 2 as a plot of μ' versus temperature. This transition is representative of the others except for $x=0.9$ where a second small but equally sharp transition appeared near the top of the curve, probably due to some bcc precipitate in this largely hcp sample. T_c for $x=0.31$ was obtained from specific-heat jump data. The results are all listed in Table I.

The sample heat capacity at a given temperature is obtained by subtracting the sample holder (addendum) heat capacity from the total measured heat capacity of the sample and sample holder. The heat-capacity data of all the samples are shown in Figs. 3–8 as plots of C/T versus T^2 . The normal-state parameters γ (electronic specific-heat coefficient), β (related to Debye lattice heat capacity), and α (contribution from the presence of T^5 term in lattice heat

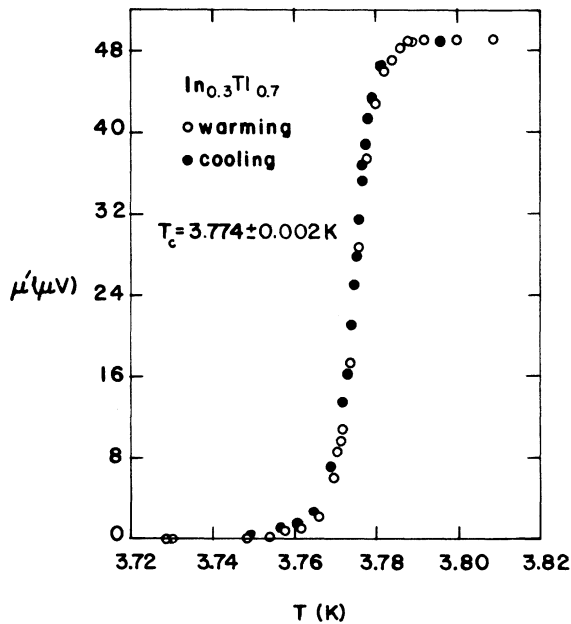


FIG. 2. ac permeability μ' (in μV) vs temperature T (K) for the $x=0.7$ sample on passing through the superconducting transition. The values for T_c and the width of the transition are discussed in the text.

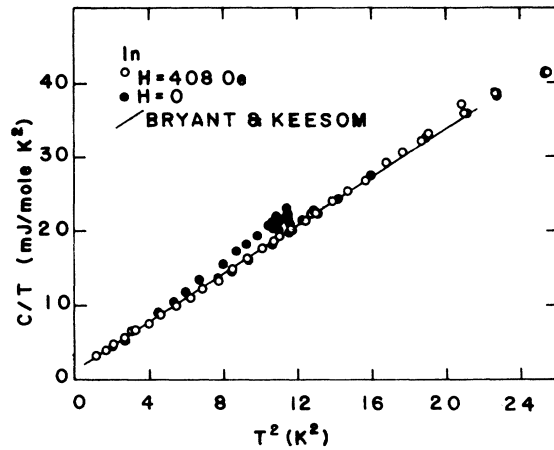


FIG. 3. The molar specific heat of In plotted as C/T vs T^2 . The solid line is a plot of the data of Ref. 7.

capacity) were obtained from the measured molar heat-capacity data by a weighted least-squares fit to the expression

$$C/T = \gamma + \beta T^2 + \alpha T^4,$$

where C is in $\text{mJ}(\text{mole})^{-1} \text{K}^{-1}$ and β is given in terms of the Debye temperature, Θ_D , by

$$\beta = 12\pi^2 R / 5\Theta_D^3 = 1.9437 \times 10^6 / \Theta_D^3 \text{ mJ/mole K}^4.$$

where R is the gas constant.

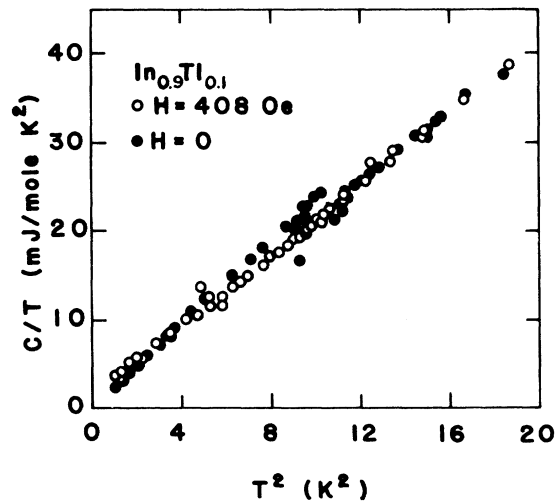


FIG. 4. The molar specific heat of the $x=0.1$ sample plotted as C/T vs T^2 .

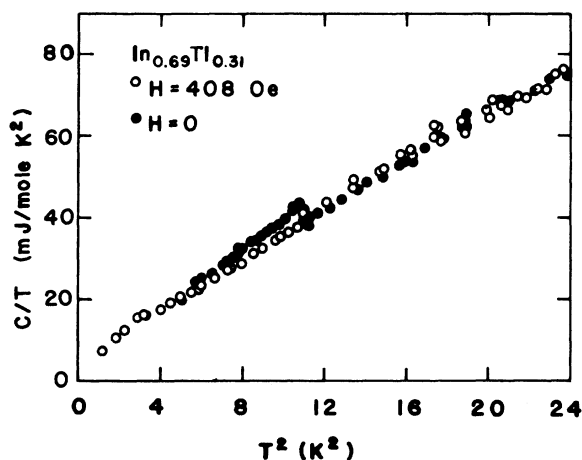


FIG. 5. The molar specific heat of the $x = 0.31$ sample plotted as C/T vs T^2 .

For samples $x = 0.31$ and 0.35 the heat-capacity data below 2 K were not taken into consideration for the least-squares fit because of an indication of a small transition taking place, as seen in Figs. 5 and 6. A probable reason for observing this small transition at low temperatures is that our solenoid was incapable of producing sufficient magnetic field to quench the superconductivity completely. In the case of the sample $x = 0.7$, heat-capacity data below 3 K were not included in the least-squares fit for the same reason. For this particular sample, there is considerable uncertainty in γ and Θ_D values because of omitting the low-temperature data. The uncertainties quoted in Table I for γ and Θ_D are one standard deviation of

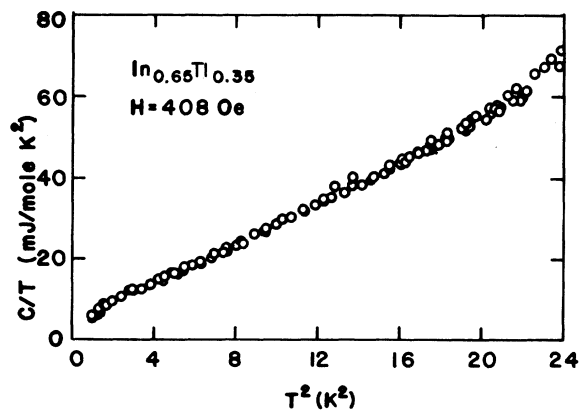


FIG. 6. The molar specific heat of the $x = 0.35$ sample plotted as C/T vs T^2 .

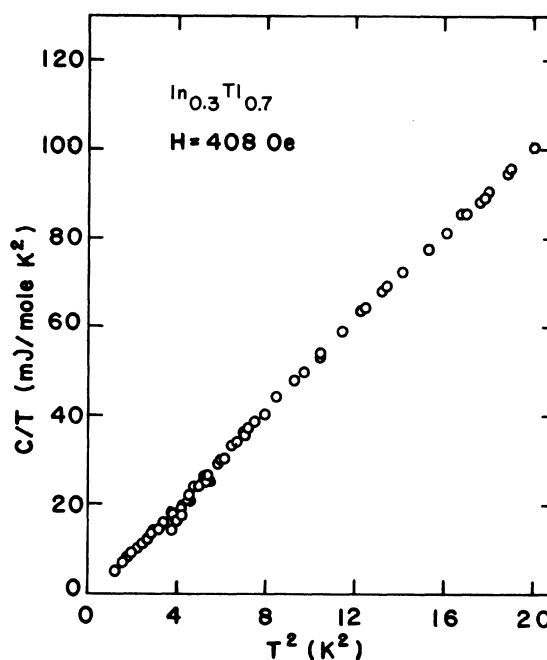


FIG. 7. The molar specific heat of the $x = 0.70$ sample plotted as C/T vs T^2 .

the mean calculated from the least-squares-fit matrix. Also included in Table I are values of the reduced specific-heat jump, where measured.

IV. DISCUSSION

The sharp and single superconducting transitions of the alloys and the good agreement of their T_c 's with previous results² indicate that the samples are homogeneous and that their nominal compositions may be

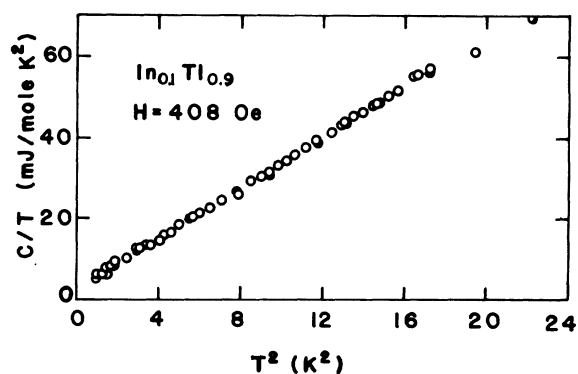


FIG. 8. The molar specific heat of the $x = 0.90$ sample plotted as C/T vs T^2 .

taken as the prepared sample compositions. In the case of $x = 0.9$, from our susceptibility measurements we estimated that about 96% of the sample is hcp and 4% of the sample is bcc. Reasonable agreement is found between susceptibility and jump T_c 's, as shown in Table I.

One of the important quantities that can be extracted from normal-state parameters is the band-structure density of states at the Fermi surface per spin per atom, $N_{BS}(0)$ which is given by

$$N_{BS}(0) = 3\gamma[2\pi^2k_B^2(1 + \lambda)]^{-1} . \quad (1)$$

In order to calculate $N_{BS}(0)$, we used γ obtained from our normal-state heat-capacity measurements and λ , obtained by interpolating at our x values the results from Dynes's tunneling measurements. The values of $N_{BS}(0)$ for our samples and the corresponding λ values taken by interpolation from Dynes's work are given in Table III. Comparison of our measured $N_{BS}(0)$ with an appropriate theory could not be done due to lack of band-structure calculations for these alloys. But some of the values appear to be remarkably high for these p -band metals.

Dynes's paper on this alloy system showed that the behavior of T_c is described very well by McMillan's equation using tunneling data to obtain the parameters λ , μ^* , and $\langle\omega\rangle$ within it. Interpolating these quantities at our x values from Dynes's data and applying McMillan's equation leads to T_c values in agreement with our measured ones comparable to that found in Dynes. The values are given in Table II. In this paper we turn our attention to the behavior of the electron-ion interaction which may be obtained from the data using our $N_{BS}(0)$ results in conjunction with Dynes's data.

Taylor and Vashishta⁹ have shown that for an alloy the first moment of the weighted phonon distribution α^2F (Ref. 4) is

$$\begin{aligned} \alpha^{(1)} &= \int_0^\infty d\omega \omega \alpha^2(\omega) F(\omega) \\ &= \frac{1}{4} N_{BS}(0) k_F^{-2} \sum_{i=1}^N (v_{si}^2)_{av} / NM_i , \end{aligned} \quad (2)$$

where k_F is the Fermi wave vector, and M_i and $(v_{si}^2)_{av}$ are the mass and averaged screened pseudopotential form factor of the ion at the i th lattice site. This equation is exact in the sense that in the calculation leading up to it such effects as short-range order, anharmonicity, and force-constant variations disappear. The sum involves no configuration averaging. The equation is inexact in the sense that the pseudopotential form factor appears rather than another form of the electron-ion matrix element and that a spherical Fermi surface is assumed. Hence it should be useful in the nearly-free-electron metals considered here.

The expression for the screened form factor is

$$(v_s^2)_{av} = \int_0^{2k_F} dq q^3 v_s^2(q) . \quad (3)$$

Employing the fact¹⁰ that for any reasonable choice of dielectric function $v_s(0) = -Z/N_{FE}(0)$, where Z is the ionic valence, it is convenient to recast Eq. (2) into the dimensionally more transparent terms of McMillan in which

$$\langle v_s^2 \rangle = \int_0^{2k_F} dq q^3 v_s^2(q) / \int_0^{2k_F} dq q^3 v_s^2(0) . \quad (4)$$

Then Eq. (2) becomes

$$\begin{aligned} 2\alpha^{(1)} &= \lambda \langle \omega^2 \rangle \\ &= (1.51/r_s) [N_{FE}(0)/N_{BS}(0)] \left[\sum_{i=1}^N \Omega_{pi}^2 \langle v_{si}^2 \rangle / N \right] . \end{aligned} \quad (5a)$$

Here r_s is the radius measured in Bohr radii of the sphere containing one electron, $N_{FE}(0) = 3Z/4E_F$ is the free-electron density of states per spin per atom, and $\Omega_{pi}^2 = 4\pi e^2 Z_i^2 / M_i \Omega$ is a convenient plasma frequency parameter for the ion at site i . Ω is the measured volume per atom in the alloy,¹¹ and $\langle \omega^2 \rangle$ is a second moment of the weighted phonon distribution defined by McMillan.

For elements Eq. (5a) reduces to

$$\lambda \langle \omega^2 \rangle / \Omega_p^2 = (1.51/r_s) [N_{FE}(0)/N_{BS}(0)] \langle v_s^2 \rangle , \quad (5b)$$

TABLE II. Comparison of measured T_c and T_c calculated by McMillan's equation.

Thallium conc. x	$\hbar \langle \omega \rangle / k_B^a$ (K)	μ^{*a}	λ^a	T_c (calc) (K)	T_c (expt) (K)
0.0	80.1	0.125	0.834	3.46	3.405
0.10	74.9	0.122	0.850	3.44	3.276
0.31	67.2	0.126	0.920	3.53	3.286
0.35	67.2	0.128	0.885	3.23	3.129
0.70	52.5	0.110	1.115	4.10	3.774
0.90	55.7	0.128	0.925	2.92	2.945
1.00	57.7	0.127	0.780	2.11	2.38

^aInterpolated from the data of Ref. 3.

which is similar to the result obtained by McMillan [Eq. (40) of Ref. 4] except for a correction factor to account for the departure of $N_{BS}(0)$ from the free-electron value.

Equation (5a) is interesting because it allows experimental determination in alloys of the behavior of the pseudopotential in that environment since all other quantities are amenable to experiment or calculation. Dynes has measured the moment, and we have determined $N_{BS}(0)$ in this work.

If one uses Eq. (5b) to calculate $\langle v_s^2 \rangle$ from measured values of the remaining parameters for In the result is $\langle v_{s_{In}}^2 \rangle = 0.0248$. This is smaller than the value 0.042 obtained from Animalu's results for the Heine-Abarenkov model potential as listed in Harrison's book¹² by a factor $F = 1.71$. The discrepancy is roughly equal to the density of states ratio in Eq. (5b); i.e., the free-electron expression would give better agreement. To proceed we arbitrarily multiply $\lambda \langle \omega^2 \rangle$ in Eq. (5) by $F = 1.71$ in order to produce coincidence for pure In:

$$F\lambda \langle \omega^2 \rangle = (1.51/r_s) [N_{FE}(0)/N_{BS}(0)] \times \left[\sum_{i=1}^N \Omega_{pi} \langle v_{si}^2 \rangle / N \right] \equiv J \quad (6)$$

In Fig. 9 we plot λ , $\hbar^2 \langle \omega^2 \rangle$, and $N_{BS}(0)$. We note that λ correlates with $N_{BS}(0)$ and oppositely with $\hbar^2 \langle \omega^2 \rangle$ as occurs in many alloy systems. The anticorrelation of $\hbar^2 \langle \omega^2 \rangle$ and $N_{BS}(0)$ is a general result

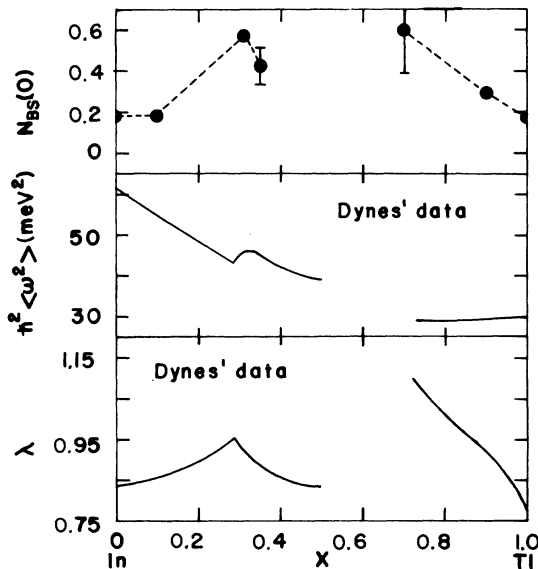


FIG. 9. λ , $\hbar^2 \langle \omega^2 \rangle$ (meV²), and $N_{BS}(0)$ (states/eV spin atom) vs x . The solid lines are smooth curves drawn through Dynes's data, Ref. 3. Note the suppression of zero on all but the top scale.

which is a consequence of the greater electronic screening of the ion-ion interaction in the higher $N_{BS}(0)$ alloys.

A plot of $F\lambda \langle \omega^2 \rangle$ is shown in Fig. 10. The remarkable feature here is the near linearity of the result apart from minor variations in the different crystal phases. The drop by a factor of 2 in going from In to Tl is clearly a mass-related effect. Roughly speaking the result in Fig. 10 is an example of the effect noticed by McMillan⁴ that $M \langle \omega^2 \rangle \lambda \approx C$, a constant for a given "class" of materials. It is noticeable that the deviations from linearity correlate with $N_{BS}(0)$.

The result shown in Fig. 10 is especially striking in light of the measured variation of $N_{BS}(0)$ (Fig. 9) which reaches up to three times the elemental values. It is apparently the case that the pseudopotential terms of Eq. (6) are proportional to $N_{BS}(0)$ so that J entails considerable cancellation.

To see how this arises it is necessary to consider the behavior of the screened pseudopotential. Since we are interested mainly in how it varies with $N_{BS}(0)$ we make a simple model for J , namely, we set

$$J = [(1-x) \Omega_{Inx}^2 \langle v_{s_{In}}^2 \rangle_x + x \Omega_{Tlx}^2 \langle v_{s_{Tl}}^2 \rangle_x] \times (1.51/r_s) [N_{FE}(0)/N_{BS}(0)]_x \quad (7)$$

where all quantities are calculated using parameters measured for alloy x and, in particular, the pseudopotential form factors are screened in accordance with measured $N_{BS}(0)$ in the alloy of concentration x .

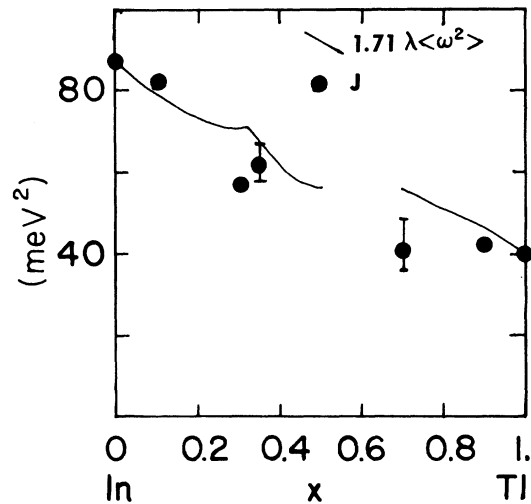


FIG. 10. $1.71\lambda \langle \omega^2 \rangle$ and J vs Tl concentration x . The solid lines are smooth curves passing through points calculated from Dynes's (Ref. 3) data. The dots are calculated from Eq. 7. The error bars represent propagation of the uncertainty in $N_{BS}(0)$ where it was larger than the dots. The data are in meV².

For convenience we use Ashcroft's¹³ empty-core bare pseudopotential which has only the core radius R_c as an adjustable parameter, and the Hubbard-Sham¹⁴ form of the dielectric function for the free-electron gas which includes an accounting of exchange and correlation. The screened pseudopotential form factor is thus¹⁵

$$v_s(q) = -4\pi Ze^2 \Omega^{-1} q^{-2} \cos(R_c q) / \epsilon(q) ,$$

where Ω is the atomic volume and

$$\epsilon(q) = 1 + (\lambda_T/q)^2 u(q) [1 - G(q)] .$$

Here $u(q)$ is the Lindhard function and

$$G(q) = \frac{1}{2} q^2 (q^2 + k_F^2 + \frac{1}{2} \lambda_T^2)^{-1}$$

corrects for exchange and correlation.¹⁶ λ_T is the Fermi-Thomas screening wave vector, $\lambda_T^2 = 8\pi e^2 N_{BS}(0)/\Omega$. Introducing the dimensionless wave-vector variable $y = q/2k_F$ and parameters $B = \lambda_T/2k_F$ and $A = 2k_F R_c$ the integrals of Eq. (4) are written as

$$\langle v_s^2 \rangle = \int_0^1 4B^4 y^{-1} \cos^2(Ay) \times \{1 + (B/y)^2 u(y) [1 - G(y)]\}^{-2} dy . \quad (8)$$

This is easily evaluated numerically.

The procedure is to fix A for the elemental end points using the measured $N_{BS}(0)$ to evaluate B and Eq. (6) to evaluate $\langle v_s^2 \rangle$ there. This scheme gives $R = 0.524 \text{ \AA}$ for In and $R = 0.567 \text{ \AA}$ for Tl. Then, using the same R_c values for the elements within the alloy, one evaluates J from Eq. (7) for the alloy. The results are shown for our samples in Fig. 10 and listed in Table III. One can see that the scheme works: J is indeed quite insensitive to $N_{BS}(0)$. However, there is considerable disagreement between calculated and measured results. In fact the calculated points deviate most negatively from linearity where the measured ones deviate most positively and vice versa so that the calculated ones tend to anticorrelate with $N_{BS}(0)$.

The elimination of the arbitrary factor of $F = 1.71$ in Eq. (6) does not change the general result that $\langle v_s^2 \rangle$ tends to cancel $N_{BS}(0)$, but one is forced to adopt unreasonable parameters to get a fit.

The result can be stated in another way. This experiment presents evidence that the behavior of $\langle v_s^2 \rangle$ for an element within an alloy is governed mainly by one factor: the electron density of states; and $\langle v_s^2 \rangle / N_{BS}(0)$ is nearly constant.

The results in these In-Tl alloys are similar to those by Dynes and Rowell¹⁷ in Tl-Pb-Bi alloys where they found $\lambda \langle \omega^2 \rangle / \Omega_p^2$ is nearly constant. They used the free-electron version of Eq. (5b) to analyze the results since $N_{BS}(0)$ values were not available at the time. Subsequent measurements by *Hermans et al.*¹⁸

TABLE III. Measured and calculated quantities used in the analysis of this experiment. The parameters are defined and discussed in the text. The last two columns are compared in Fig. 10.

Tl conc. x	r_s	$N_{FE}(0)$ (states/eV spin atom)	$N_{BS}(0)$	$\hbar^2 \Omega_p^2 / \mu_{In}$	$\hbar^2 \Omega_p^2 / \mu_{Tl}$	$\langle v_{s_{In}}^2 \rangle / N_{BS}(0)$ (states/eV spin atom) ⁻¹	$\langle v_{s_{Tl}}^2 \rangle / N_{BS}(0)$ (states/eV spin atom) ⁻¹	λ	$\hbar^2 \langle \omega^2 \rangle$	$1.71 \hbar^2 \langle \omega^2 \rangle \lambda$ (meV ²)	J
0	2.414	0.2616	0.183 ± 0.021	2265	1272	0.235	0.196	0.834	61.17	87.1	87.1
0.1	2.421	0.2632	0.186 ± 0.024	2244	1261	0.236	0.196	0.850	54.30	78.8	82.3
0.31	2.437	0.2666	0.571 ± 0.033	2202	1237	0.190	0.147	0.920	45.0	70.7	57.0
0.35	2.440	0.2672	0.421 ± 0.086	2194	1233	0.212	0.168	0.885	45.0	68.0	62.0
0.70	2.465	0.2728	0.604 ± 0.211	2127	1195	0.191	0.147	1.115	29.2	55.6	40.9
0.90	2.479	0.2759	0.294 ± 0.017	2091	1175	0.236	0.192	0.925	29.5	46.6	42.4
1.0	2.486	0.2775	0.175 ± 0.002	2073	1165	0.243	0.204	0.780	30.13	40.1	40.1

show $N_{BS}(0)$ to vary only by 10% over the alloy range measured. We may take our results here to indicate that even where $N_{BS}(0)$ is varying rapidly so that Eq. (5a) should be used the electronic portion of λ is slowly varying.

Finally, some remarks on the martensitic transition. To observe this at low temperatures we prepared the $x = 0.31$ sample, because this is the concentration at which Merriam *et al.* show a T_c discontinuity. The idea was to observe a jump or other anomaly in the specific heat at the martensitic transition temperature T_m similar to that observed in V_3Si .¹⁹ We saw no such jump, which was expected to occur around 3 K. The specific-heat data of this sample both in zero field and in a 408 Oe field are shown in Fig. 5. By carefully observing the data it may be seen that above the superconducting transition there is considerable scatter between $T^2 = 17$ and 21 K^2 . It is possible that this scatter represents a smeared martensitic transition in this polycrystalline sample which was probably inhomogeneously strained by mounting in the sample holder. We also attempted to mount the sample in a strain-free way in a sealed capsule filled with He gas for thermal contact. The thermal contact was so poor that any transition which might have occurred was swamped by the noise of our data (which are not shown here.) It is also possible that the expected transition did not oc-

cur over the measured temperature range, perhaps because of supercooling.

V. CONCLUSIONS

In the superconducting transition temperatures of In-Tl bulk alloys and in the low-temperature normal-state specific heat of In our measurements agree very well with those of other workers. The band-structure electron density of states taken from our specific-heat measurements behaves qualitatively like T_c and λ along the alloy series. Surprisingly it reaches values of up to three times the elemental values.

The results of Dynes's work have been used to probe the behavior of $\lambda(\omega^2)$ which was found to decrease nearly linearly by a factor of 2 in going from In to Tl. This is in spite of several crystal phase changes and the large variation in $N_{BS}(0)$. We show this to be mainly a consequence of the fact that $\langle v_s^2 \rangle / N_{BS}(0)$ is calculated to be nearly constant for each element within the alloy.

Finally, a specific-heat anomaly associated with an expected martensitic transition at $\sim 3 \text{ K}$ in the $\text{In}_{0.69}\text{Tl}_{0.31}$ alloy was not observed, either because the sample was inhomogeneously strained and the transition smeared into the scatter in the data or, perhaps, because of supercooling beyond the measuring range of temperature.

*Based on the Ph.D. thesis of Lakshmi V. Munukutla (Ohio University, 1979) (unpublished).

†Present address: Dept. of Physics, Texas A & M University, College Station, Texas 77843.

¹M. Hansen, *Constitution of Binary Alloys* (McGraw-Hill, New York, 1958).

²M. F. Merriam, J. Hagen, and H. L. Luo, *Phys. Rev.* **154**, 424 (1967).

³R. C. Dynes, *Phys. Rev. B* **2**, 644 (1970); **4**, 3255 (1971).

⁴W. L. McMillan, *Phys. Rev.* **167**, 331 (1968).

⁵For a review, see the articles by V. Heine, M. L. Cohen, and D. Weaire, in *Solid State Physics*, edited by H. Ehrenreich, R. Seitz, and D. Turnbull (Academic, New York, 1970), Vol. 24.

⁶D. K. Finnemore and D. E. Mapother, *Phys. Rev.* **140**, A507 (1965).

⁷C. A. Bryant and P. H. Keesom, *Phys. Rev.* **123**, 491 (1961).

⁸B. J. C. van der Hoeven, Jr., and P. H. Keesom, *Phys. Rev.* **135**, A631 (1964).

⁹D. W. Taylor and P. Vashishta, *Phys. Rev. B* **5**, 4410 (1972).

¹⁰L. J. Sham and J. M. Ziman, *Solid State Phys.* **15**, 221 (1963).

¹¹R. W. Meyerhof and J. F. Smith, *Acta Metall.* **2**, 529 (1963).

¹²W. A. Harrison, *Pseudopotentials in the Theory of Metals* (Benjamin, Massachusetts, 1966), p. 313.

¹³N. W. Ashcroft, *Phys. Lett.* **23**, 48 (1966).

¹⁴L. J. Sham, *Proc. R. Soc. London Ser. A* **283**, 33 (1965).

¹⁵The discussion here follows M. L. Cohen and V. Heine, *Solid State Phys.* **24**, 37 (1970).

¹⁶Other expressions for $G(q)$ give values of $\langle v_s^2 \rangle$ differing by a few percent from the Sham form, e.g., K. S. Singwi, A. Sjölander, M. P. Tosi, and R. H. Land, *Phys. Rev. B* **1**, 1044 (1970); P. Vashishta and K. S. Singwi, *Phys. Rev. B* **6**, 875, 4883 (1970).

¹⁷R. C. Dynes and J. M. Rowell, *Phys. Rev. B* **11**, 1884 (1975).

¹⁸F. Hermans, J. C. Ho, J. Boyer, and N. E. Phillips, *J. Phys. (Paris) Suppl.* **39**, C6-477 (1978).

¹⁹J. E. Kunzler, J. P. Maita, H. J. Levenstein, and E. J. Ryder, *Phys. Rev.* **143**, 390 (1966)